PHYSICAL REVIEW B VOLUME 40, NUMBER 14 15 NOVEMBER 1989-I

Determination of the local order in amorphous cobalt films

H. Magnan
Laboratoire pour l'Utilisation du Rayonnement Électromagnétique, Université de Paris Sud, F-91405 Orsay CEDEX, France and Service de Physique des Atomes et des Surfaces, Centre d'Etudes Nucléaires, F-91191 Gif Sur Yvette CEDEX, France

D. Chandesris and G. Rossi
Laboratoire pour l'Utilisation du Rayonnement Électromagnétique, Université de Paris Sud, F-91405 Orsay CEDEX, France

G. Jezequel
Laboratoire pour l'Utilisation du Rayonnement Électromagnétique, Université de Paris Sud, F-91405 Orsay CEDEX, France and Laboratoire de Spectroscopie, Université de Rennes, F-35042 Rennes CEDEX, France

K. Hricovini*
Laboratoire pour l'Utilisation du Rayonnement Électromagnétique, Université de Paris Sud, F-91405 Orsay CEDEX, France

J. Lecante
Laboratoire pour l'Utilisation du Rayonnement Électromagnétique, Université de Paris Sud, F-91405 Orsay CEDEX, France and Service de Physique des Atomes et des Surfaces, Centre d'Etudes Nucleaires, F-91191 Gif Sur Yvette CEDEX, France

(Received 8 September 1989)

The local atomic structure of amorphous cobalt films prepared by vapor condensation on a low-temperature substrate is determined by extended x-ray-absorption fine structure. The deduced radial distribution function corresponding to the first shell of neighbors is broadened compared to that of crystalline cobalt and is asymmetrical. The measured profile allows us to conclude the existence of a true amorphous monometallic sample and compares well with the calculated one assuming a random packing of hard spheres. The existence domain of this structure is then outlined.

The question of the stabilization of a pure amorphous transition-metal film has been open for many years.[1] The knowledge of the atomic structure of amorphous monometallic transition metals is fundamental for the understanding of their remarkable electronic and magnetic properties[2] and it represents the starting point for the determination of the microscopic phenomenology of crystallization.

Although studies have been carried out on various classes of amorphous metallic alloys, very little is known about the amorphous phase of transition metals. We present in this paper the first direct analysis of the local crystallographic environment of low-temperature condensed cobalt films prepared in ultrahigh vacuum; moreover, we followed its evolution with temperature.

In contrast to the large theoretical effort which has been devoted to the modeling of the amorphous state of pure metals, the experimental information is scarce due to the difficulty of the sample preparation and characterization. The objective of the structural models[3,4] was to fit the general shape of the radial distribution function (RDF) deduced from electron diffraction studies on different monometallic amorphous samples:[5–7] it is characterized by a well-defined first shell and a second shell divided in two components. However, these structural experiments are not sensitive to the shape of the first shell: Different extended x-ray-absorption fine-structure (EXAFS) studies on amorphous metallic alloys have determined an asymmetrical first shell of neighbors which can be simulated by the superposition of two Gaussian profiles,[8] while the classical neutron or x-ray diffraction experiments on the same samples lead to a first-shell profile which is an average value of the asymmetrical RDF obtained by EXAFS. Up to now no EXAFS study has been done on monometallic amorphous samples since they need a high vacuum and a low-temperature environment. The surface EXAFS setup[9] available at the Laboratoire pour l'Utilisation du Rayonnement Electromagnétique (LURE) enabled us to do this experiment. Moreover the use of electron collection to record x-ray-absorption spectra allows us to study amorphous cobalt films of different thicknesses (2 to 100 Å) and on different substrates.

Previous studies have shown that when a cobalt film is prepared by low-temperature condensation it exhibits an amorphouslike structure.[5,10,11] Moreover temperature-dependent measurements have shown a drop in the resistivity (at about 38 K) for such an amorphous cobalt (*a*-Co) sample prepared at 4 K. A simultaneous measurement of the resistivity and a scanning electron diffraction study of thin films allowed Leung and Wright[6] to attribute this change to a crystallization into a microcrystalline structure. The temperature of this transition is strongly dependent on the impurity content of the sample. The EXAFS study presented here also allows a precise determination of the evolution of the local atomic structure of these amorphous films as the temperature is increased.

The cobalt is evaporated from a high purity cobalt wire

heated by electron bombardment in a vacuum never exceeding 5×10^{-10} mbar (base pressure is 2×10^{-10} mbar). It is deposited at a rate of about 10^{12} atoms/cm^{2}s on a thin glass slide glued with silver paint on the copper end of a helium flow cryostat. The temperature measured with a Pt resistor glued in a small hole in the copper is below 20 K and no modification is observed during evaporation thanks to the use of a radiation shielding. The evaporation rate is calibrated prior to the evaporation with a quartz microbalance. Then the thickness of the film is checked by measuring the x-ray-absorption edge jump of the sample at the cobalt K edge. Using this calibration, we estimate the thickness of the grown film with an accuracy of 10% (the films are assumed to be homogeneous). The local atomic structure of the films is then studied with EXAFS spectra which are recorded at low temperature even for the annealed samples in order to avoid differences in the thermal disorder.

The surface EXAFS experiments are performed at LURE on the Dispositif de Collisions dans l'Igloo (DCI) storage ring at Orsay with a Si(311) double-crystal monochromator. The variations of the x-ray-absorption coefficient of the sample are measured above the K edge (7709 eV) of cobalt in the total yield mode. Experimental spectra recorded on a 50-Å film of cobalt are represented in Fig. 1(a) both for the sample just after its preparation (20 K) and after an annealing of 5 min at 120 K. Relevant steps of the EXAFS analysis are displayed in Figs. 1(b) and 2. The Fourier transform for the annealed sample is very similar to that of bulk cobalt; for the low-temperature sample it has the typical shape usually found for an amorphous structure:[8,12] shorter distance and lower amplitude for the first shell, quasiabsence of more distant shells.

The usual formula giving the EXAFS modulation function χ for a monoatomic disordered system with a radial distribution function $F(r)$ is:[13]

$$\chi(k)=\int B^*(k)[P(r)/k]\sin[2kr+\delta(k)]dr\,,$$

where $P(r)=F(r)/r^2$ is an "effective distribution" since $F(r)$ is the probability of finding the neighbor of the absorbing atom in the range r to $r+dr$ including static and thermal disorder. $B^*(k)=B(k)\exp(-2r/\lambda)$, where λ is the mean free path of the photoelectron, k its wave number, and $B(k)$ the backscattering amplitude. In the analysis of the first shell of neighbors we will approximate $\exp(-2r/\lambda)$ by its mean value on this shell, $\exp(-2\langle r\rangle/\lambda)$, and assume that this term is identical in the amorphous and in the crystalline cobalt samples. $[2kr+\delta(k)]$ is the total phase shift taking into account atomic potentials.

The first-shell distribution function is asymmetrical in systems in which the static arrangement of the atoms is described as a dense random packing of hard spheres.[4] Eisenberger and Brown have shown[13] that if the standard EXAFS formula assuming a Gaussian RDF is used to fit data of a system in which the effective distribution function is asymmetric, incorrect values are obtained both for distances and coordination numbers. One solution to this problem is to use the cumulant expansion approach to EXAFS data analysis introduced by Bunker;[14] the first

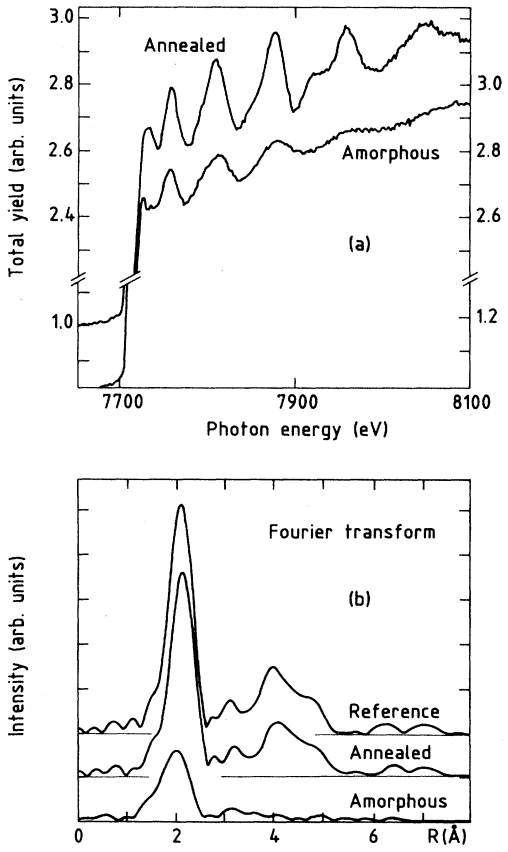

FIG. 1. (a) EXAFS spectra of a 50-Å-cobalt film as condensed on a glass substrate at $T<20$ K (lower curve) and after an anneal of 5 mn at 120 K. Both spectra are recorded at 20 K. (b) The same data after Fourier transform between $k=3.1$ Å^{-1} and $k=11.1$ Å^{-1} (lower curve, as evaporated; middle curve, annealed film) and reference Fourier transform of hcp cobalt (upper curve).

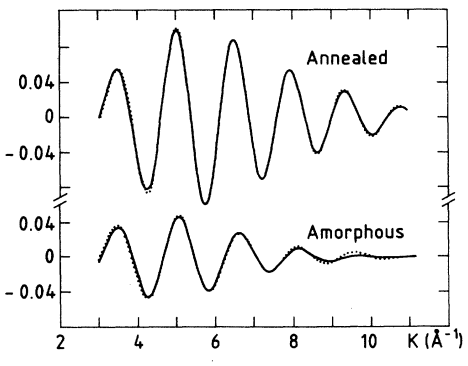

FIG. 2. The dotted curves are inverse Fourier transforms of the first shell for the annealed and unannealed 50-Å film (upper and lower part). The continuous curves are calculated using cumulants deduced from the analysis of these data (see text).

cumulants are:

$$C_0 = \ln\left[\int P(r)dr\right],$$

$$C_2 = \int (r-\bar{r})^2 P(r)dr \Big/ \int P(r)dr,$$

$$C_3 = \int (r-\bar{r})^3 P(r)dr \Big/ \int P(r)dr,$$

where $\bar{r} = \int rP(r)dr / \int P(r)\,dr$ is the centroid of the effective distribution. Third- and higher-order cumulants measure the deviation of $P(r)$ from a Gaussian distribution. If we just consider the first term of this deviation C_3 which measures the asymmetry of the distribution, the EXAFS formula for the first shell becomes:

$$k\chi(k) = A(k)\sin\Phi(k), \quad (1)$$

where $A(k) = B^*(k)\exp(C_0 - 2C_2k^2)$ and $\Phi(k) = \delta(k) + 2k\bar{r} - [(2k)^3/3!]C_3$.

As a reference, we use the EXAFS spectrum recorded at 20 K of a 60-Å-thick film of cobalt annealed at 500 K. The first shell of neighbors in hcp cobalt consists of two atoms at 2.48 Å, four at 2.50 Å, six at 2.51 Å, and a Debye-Waller factor at 20 K of 0.0027 Å^2;[15] we can approximate it by a single shell of $N_{\text{ref}} = 12$ atoms at $R_{\text{ref}} = 2.50$ Å with the same Debye-Waller factor σ^2_{ref}. Then

$$k\chi_{\text{ref}}(k) = (N_{\text{ref}}/R^2_{\text{ref}})B^*(k)\exp(-2k^2\sigma^2_{\text{ref}}) \times \sin[2kR_{\text{ref}} + \delta(k)] = A_{\text{ref}}(k)\sin\Phi_{\text{ref}}(k).$$

The local environment of the different samples is determined by a ratio method. We plot $\ln[A(k)/A_{\text{ref}}(k)]$ and $\Phi(k) - \Phi_{\text{ref}}(k)$ vs k^2 and k, respectively, for an independent determination of the cumulants by a polynomial fit in the k range 3–8 Å^{-1}. These cumulants are used to calculate $k\chi(k)$ from Eq. (1); the result is then compared to the filtered EXAFS spectrum. This comparison is done in Fig. 2 for both the amorphous recrystallized 50-Å film. The experimental values for different films are given in Table I, N is the number of first neighbors and $\langle R\rangle$ the mean r value on the RDF $[\langle R\rangle = (\bar{r}^3 + 3\bar{r}C_2 + C_3)/(\bar{r}^2 + C_2)]$. Then the cumulants are used to construct the RDF.[16,17] These first-shell RDF are shown in Fig. 3 for the crystallized sample and two amorphous films of different thicknesses: 12 and 50 Å. All the amorphous samples RDF's that we have measured are very similar which means that this profile is characteristic of a-Co. By comparing it with the crystalline sample RDF one can conclude that when going from the crystallized to the amorphous sample (i) the maximum RDF value decreases by a factor of 2.3, (ii) the full width at half maximum increases by a factor of 2.1, (iii) the shape becomes very asymmetrical: the RDF has a steep edge for the short distances and a skewed profile at longer distances (the third cumulant C_3 is positive). This is the first experimental determination of the asymmetry of the first shell in a monometallic amorphous sample. The monometallic nature of our samples render the quantitative determination of the asymmetry of the first shell all the more precise due to the presence of just one kind of neighbor. The first-neighbor distance and coordination number deduced from electron diffraction[6] are equal to the average values $\langle R\rangle$ and N that we have measured.

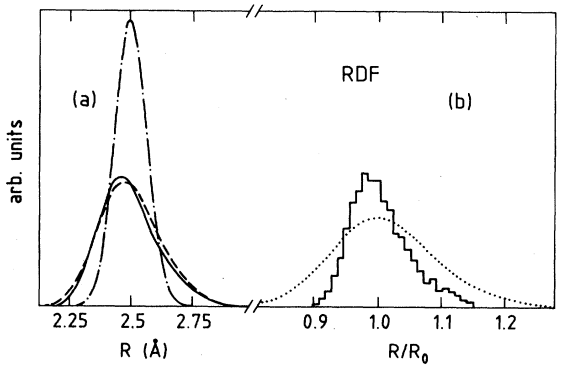

FIG. 3. (a) Radial distribution function of the first shell as derived from the experiment: dashed and dashed-dotted lines are for the amorphous and annealed 50 Å film, respectively, solid line for the 12 Å amorphous film; (b) RDF of the first shell calculated by Heimendahl (Ref. 4) (solid line) and by Baer *et al.* (Ref. 18) (dotted line).

The question now is "how does this measured RDF profile compare with the different models?" First, it clearly excludes all the descriptions of these films as microcrystallites: indeed, in a microcrystalline structure we expect a RDF first-shell peak which is not broadened as compared to the crystalline structure. Different models were adjusted in order to fit the a-Co RDF deduced from electron diffraction studies by Leung and Wright,[6] and in particular to reproduce the position and shape of the second split peak and of the third peak. One of them is the structural diffusion model (SDM) developed recently by Baer *et al.*[18] Their idea is that the short-range order in amorphous systems has remnants of the directly competing crystalline structure; so they have started their SDM

TABLE I. Structural parameters results of polynomial fits for three different films compared to these deduced from the electron diffraction experiment by Leung and Wright (Ref. 6).

Sample	N	$\bar{r}$ (Å)	C_2 (10^{-3} Å^2)	C_3 (10^{-3} Å^3)	$\langle R\rangle$ (Å)
Film 12 Å	9.5 ± 1	2.49 ± 0.02	13 ± 2	1.8 ± 0.5	2.50 ± 0.02
Film 50 Å	10 ± 1	2.49 ± 0.02	15 ± 2	1.4 ± 0.5	2.50 ± 0.02
Annealed 50 Å	12 ± 0.5	2.50 ± 0.01	4 ± 1	0 ± 0.2	2.50 ± 0.01
Ref. 6	11				2.49

calculation with a fcc crystallographic unit cell which is then distorted by keeping bond lengths and two of the internal angles fixed. The RDF of the first-shell calculated with this model using the parameters determined by Baer *et al.*[18] is given [Fig. 3(b)]: it is much broader than the experimental profile and does not present the steep edge for the short distances which is deduced unambiguously from the EXAFS measurements.

Another *a*-Co RDF calculation was previously developed by Heimendahl[4] using a model based on a dense random packing of hard spheres relaxed with respect to a realistic interatomic potential. In addition to a good reproduction of the diffraction results for the second and third shells, the first coordination shell profile is precisely calculated in the model; it could not be compared to earlier experimental data since electron diffraction is not accurate enough to give the first-shell profile. One can see in Fig. 3 that the agreement between Heimendahl's model and the EXAFS data is very good: both the width and the asymmetry of the first shell were correctly predicted. So we show here the accuracy of the hard-spheres model to describe the local structure of an amorphous monometallic sample; moreover, we point out that the precise determination of the shape of the first shell which is allowed by EXAFS is necessary to discriminate between different models which fit higher-shells RDF equally well.

We have explored the range of stability of *a*-Co films with respect to film thickness, annealing temperature, and substrate. Previous studies showed that amorphous films of Fe and Ni can be prepared by low-temperature condensation only for thicknesses below a critical value: 150 Å (Ref. 6) or 50 Å (Ref. 19) for Fe, 30 Å (Ref. 7), or always crystalline (Ref. 6) for Ni. No critical thickness behavior has been reported up to now for *a*-Co.[10] In our experiment the higher thickness obtained for amorphous films prepared on glass substrate is 50 Å even at the lowest temperature. Furthermore, on a substrate which favors the epitaxial growth like Cu(111) (Refs. 9 and 17), we could not grow amorphous Co films of any thickness. The role of the interface structure appears therefore to be crucial in the stabilization of the amorphous structure of very clean thin films.

By following the evolution of the Co short-range order after different annealing steps we observe three different stages: (i) in a first range of temperature, the spectrum is unchanged; (ii) in a second one, there is a sharp increase of the height of the first shell in the Fourier transform; in a range of about 10 K it reaches its bulk value; (iii) in a third range the intensities of the higher shells converge slowly to their bulk values. This can be understood as an orientational ordering which mainly affects these shells. The temperature of the second stage (which is the beginning of crystallization) is highly dependent on the thickness of the sample: It decreases continuously from 220 to 110 K for thicknesses increasing from 10 to 50 Å.[17] This behavior consistent with the existence of a critical thickness shows the deciding role of the interfaces in the stabilization of the amorphous structure in these very clean films. It can be compared to the role of the implanted metalloid atoms in the stability of amorphous metals.[20]

In conclusion, we have measured with EXAFS the asymmetry of the first-shell RDF in thin *a*-Co films condensed at 20 K in ultrahigh vacuum. The as-determined profile, broadened with respect to the crystal and highly asymmetric, allows us to affirm that these films have a true amorphous structure which can be described by a relaxed random close packing of hard spheres. We have studied the existence domain of this structure as a function of the substrate, the film thickness, and temperature.

The Laboratoire pour l'Utilisation du Rayonnement Electromagnétique is Laboratoire mixte du Centre Nationale de la Recherche Scientifique, Commissariat à l'Énergie Atomique et Ministère de l'Education Nationale.

*Permanent Address: Department of Physics, Slovak Technical University, Mlynska Dolina, 81219 Bratislava, Czechoslovakia.

[1]W. Buckel, Z. Phys. **138**, 136 (1954).

[2]G. Bergmann, Phys. Rev. Lett. **41**, 264 (1978); Gang Xiao and C. L. Chien, Phys. Rev. B **35**, 8763 (1987).

[3]J. F. Sadoc, J. Dixmier, and A. Guinier, J. Non-Cryst. Solids **12**, 46 (1973).

[4]L. v. Heimendahl, J. Phys. F **5**, L141 (1975).

[5]L. B. Davies and P. J. Grundy, Phys. Status Solidi (a) **8**, 189 (1971); J. Phys. (Paris) Colloq. **36**, C2-59 (1975).

[6]P. K. Leung and J. G. Wright, Philos. Mag. **30**, 185 (1974); **30**, 995 (1974).

[7]T. Ichikawa, Phys. Status Solidi (a) **19**, 707 (1973).

[8]A. Sadoc, D. Raoux, P. Lagarde, and A. Fontaine, J. Non-Cryst. Solids **50**, 331 (1982).

[9]P. Roubin, D. Chandesris, G. Rossi, and J. Lecante, J. Phys. F **18**, 1165 (1988).

[10]J. Wright, IEEE Trans. Magn. **MAG-12**, 95 (1976).

[11]M. R. Bennet and J. G. Wright, Phys. Status Solidi (a) **13**, 135 (1972).

[12]G. Stegemann and B. Lengeler, J. Phys. (Paris) Colloq. **47**, C8-407 (1986).

[13]P. Eisenberger and G. S. Brown, Solid State Commun. **29**, 481 (1979).

[14]G. Bunker, Nucl. Instrum. Methods **207**, 437 (1983).

[15]M. C. Desjonquères and G. Tréglia, Phys. Rev. B **34**, 6662 (1986).

[16]E. D. Crozier, J. J. Rehr, and R. Ingalls, in *X-Ray Absorption, Principles, Applications, Techniques of EXAFS, SEXAFS, and XANES,* edited by D. C. Koninsberger and R. Prins, Chemical Analysis, Vol. 92 (Wiley, New York, 1988).

[17]H. Magnan, D. Chandesris, G. Jezequel, K. Hricovini, G. Rossi, and J. Lecante (unpublished).

[18]S. Baer, E. Canessa, J. M. Lopez, and M. Silbert, Physica B **154**, 8 (1988).

[19]B. G. Lazarev, V. M. Kuz'menko, A. I. Sudovtsov, and V. I. Mel'nikov, Pis'ma Zh. Eksp. Teor. Fiz. **10**, 261 (1969) [JETP Lett. **10**, 165 (1969)].

[20]A. V. Drigo, M. Berti, A. Benyagoub, H. Bernas, J. C. Pivin, F. Pons, L. Thomé, and C. Cohen, Nucl. Instrum. Methods **B19**, 533 (1987).